Measurement of Fundamental Illite Particle Thicknesses by X-ray Diffraction Using PVP10 Intercalation

Article *in* Clays and Clay Minerals · January 1998

DOI: 10.1346/CCMN.1998.0460110

CITATIONS
99

READS
497

4 authors, including:

Vladimir Šucha
European Commission
80 PUBLICATIONS **1,353** CITATIONS

SEE PROFILE

Clays and Clay Minerals, Vol. 46, No. 1, 89–97, 1998.

MEASUREMENT OF FUNDAMENTAL ILLITE PARTICLE THICKNESSES BY X-RAY DIFFRACTION USING PVP-10 INTERCALATION

D. D. EBERL,[1] R. NÜESCH,[2] V. SUCHA[3] AND S. TSIPURSKY[4]

[1] U.S. Geological Survey, 3215 Marine Street, Boulder, Colorado 80303

[2] ETH, IGT-ClayLab, Institut für Geotechnik, Sonneggstrasse 5, CH-8092 Zürich, Switzerland

[3] Dept. of Geology of Mineral Deposits, Comenius University, Mlynská Dolina G, 842 15 Bratislava, Slovakia

[4] Nanocor, 1350 W. Shure Drive, Arlington Heights, Chicago, Illinois

Abstract—The thicknesses of fundamental illite particles that compose mixed-layer illite–smectite (I–S) crystals can be measured by X-ray diffraction (XRD) peak broadening techniques (Bertaut–Warren–Averbach [BWA] method and integral peak-width method) if the effects of swelling and XRD background noise are eliminated from XRD patterns of the clays. Swelling is eliminated by intercalating Na-saturated I–S with polyvinylpyrrolidone having a molecular weight of 10,000 (PVP-10). Background is minimized by using polished metallic silicon wafers cut perpendicular to (100) as a substrate for XRD specimens, and by using a single-crystal monochromator. XRD measurements of PVP-intercalated diagenetic, hydrothermal and low-grade metamorphic I–S indicate that there are at least 2 types of crystallite thickness distribution shapes for illite fundamental particles, lognormal and asymptotic; that measurements of mean fundamental illite particle thicknesses made by various techniques (Bertaut–Warren–Averbach, integral peak width, fixed cation content, and transmission electron microscopy [TEM]) give comparable results; and that strain (small differences in layer thicknesses) generally has a Gaussian distribution in the lognormal-type illites, but is often absent in the asymptotic-type illites.

Key Words—Bertaut, Fundamental Illite Particles, Illite, Illite–Smectite, Mixed-Layering, Peak Broadening, Polyvinylpyrrolidone, Warren–Averbach, X-ray Diffraction.

INTRODUCTION

Mixed-layer I–S crystallites that are less than 50% expandable are composed of stacks of very thin illite crystals that have water and exchange cations absorbed on their basal surfaces. Expandable interlayers in such I–S crystallites are the basal surface interfaces between adjacent illite crystals. The illite crystals that form a stack are termed fundamental illite particles (Nadeau et al. 1984b), whereas the stacks themselves are termed MacEwan crystallites (Altaner et al. 1988). The process by which coherently diffracting stacks of illite crystals and their interfaces yield an X-ray pattern for I–S is termed interparticle diffraction (Nadeau et al. 1984c).

One would like to be able to measure the thicknesses of both MacEwan crystallites and fundamental illite particles because these thicknesses and their distributions may be related to physical and chemical properties and to geologic history. Such measurements have been made on particles separated from rocks using TEM (Nadeau et al. 1984a; Merriman et al. 1990; Środoń et al. 1992; Środoń and Elsass 1994; Sucha et al. 1996; Árkai et al. 1996), and using atomic force and scanning force microscopy (Lindgreen et al. 1991; Eberl and Blum 1993). These measurements are tedious, expensive and so time-consuming that it is impractical to measure more than approximately 100 crystals per sample. This many measurements may yield an accurate mean thickness for a sample, but often are inadequate to determine an accurate distribution of thicknesses.

Thickness measurements by XRD are much more efficient, because an automated XRD scan can measure billions of nano-size crystallites in a few minutes to a few hours. Crystallite sizes then are deduced from XRD peak-broadening calculations. Two methods have been developed for measuring the thickness of MacEwan crystallites: an integral peak width method based on a modified form of the Scherrer equation (Drits et al. 1997) which measures mean thicknesses, and the BWA method, based on Fourier analysis of XRD peak shape (Drits et al. 1998) which measures mean thicknesses, thickness distributions and strain. Both methods use K-saturated, dehydrated I–S to determine the thickness of stacks of fundamental illite particles (MacEwan crystallites). The mean thickness of the fundamental illite particles themselves can be determined indirectly from either of these XRD thickness measurement techniques when combined with expandability determinations (Equation [19] in Drits et al. 1997).

This paper describes a new method for measuring mean thickness, thickness distribution and strain of fundamental illite particles directly from XRD peak broadening data. Na-saturated I–S is intercalated with a polymer (polyvinylpyrrolidone) to prevent fundamental illite particles from undergoing interparticle diffraction. This intercalation technique is based on a

Table 1. XRD thickness measurements for PVP-dispersed illite samples. Samples have been described previously in the following publications, and in references found therein: Sucha et al. (1996), Drits et al. (1997, 1998), Eberl et al. (1987) and Hunziker et al. (1986). Units are nm unless indicated otherwise.

Sample	%S XRD	$\overline{T}_e$ 001	α 001	β^2 001	$\overline{T}_e$ 002	$\overline{T}_e$ 003	$\overline{T}_e$ 005	$\overline{T}_c$	strain $(\overline{\sigma_i^2})^{1/2}$ Å	$\overline{T}$ TEM	N_{fix}	$\overline{T}_{ev}$ 001	$\overline{T}_i$ 001	$1/i$ (1/deg)
Lognormal														
AR1R	0	28.2	3.25	0.20	24.7	25.1	19.4	27.8	0.06	—	29.7	35.8	24.1	3.73
SG4	1	21.7	2.95	0.27	19.3	19.2	16.0	21.5	0.06	17.8	17.8	29.5	20.4	3.21
RM30	2	11.8	2.41	0.16	10.8	11.0	8.8	12.0	0.09	11.6	10.0	14.2	10.0	1.69
RM3	3	15.7	2.62	0.26	12.7	14.8	11.2	15.5	0.09	—	11.1	20.3	14.1	2.30
RM28	3	11.7	2.36	0.20	10.5	10.3	8.9	11.5	0.09	—	9.9	14.8	9.9	1.68
RM31	3	13.5	2.52	0.16	12.1	11.8	9.2	13.7	0.12	—	12.7	16.1	10.6	1.79
RM4	4	11.6	2.36	0.18	9.9	11.5	8.8	11.8	0.09	—	8.1	14.0	10.0	1.70
LF7	5	11.0	2.30	0.18	9.7	11.2	8.0	11.2	0.10	—	8.9	13.2	9.5	1.61
RM5	5	10.8	2.29	0.23	9.8	9.5	8.2	10.6	0.09	—	11.1	13.4	9.3	1.58
M11	5	6.3	1.71	0.28	5.4	6.1	6.6	—	N.D.	5.4	5.3	8.7	6.3	1.23
LF10	6	9.6	2.22	0.21	7.2	8.2	7.5	8.4	0.09	—	6.8	12.4	8.1	1.38
RM21	6	7.0	1.96	0.21	6.6	6.8	6.2	6.9	0.09	—	5.2	9.2	6.4	1.13
RM6	7	9.9	2.22	0.17	8.3	9.3	7.1	10	0.13	—	8.6	12.2	8.0	1.38
RM35C	7	9.3	2.13	0.21	8.1	8.1	7.2	8.9	0.09	—	6.4	10.8	7.8	1.33
M8	7	5.6	1.58	0.27	5.0	5.1	4.4	5.5	0.07	—	4.1	7.5	5.1	0.90
RM11	8	8.5	2.09	0.15	8.3	8.1	7.0	8.7	0.09	—	7.4	10.1	7.1	1.30
1603	8	6.6	1.76	0.23	6.3	5.8	5.0	6.6	0.15	4.1	3.2	8.4	5.9	0.96
RM35A	12	7.2	1.92	0.15	7.0	7.0	6.1	7.4	0.09	6.9	6.8	8.9	6.2	1.08
TRH 1/37	13	4.9	1.49	0.22	4.8	3.7	3.7	5.1	0.20	3.4	—	6.1	4.6	0.80
1602	14	5.4	1.59	0.19	5.6	5.0	4.8	5.4	0.09	3.8	2.7	6.5	4.5	0.77
ZEMP	15	4.8	1.48	0.21	4.2	4.6	4.0	4.7	0.07	—	4.5	5.9	4.3	0.73
1555	21	4.0	1.29	0.19	3.7	3.5	3.5	—	N.D.	2.7	2.4	5.2	3.2	0.58
Asymptotic														
MF59	0	13.1	2.26	0.71	8.0	9.1	9.8	9.9	0.04	—	—	22.0	N.A.	2.66
MF34	0	13.3	2.25	0.76	8.2	9.2	9.4	10.1	0.04	—	—	21.5	N.A.	2.60
MF22	0	8.7	1.84	0.63	7.0	—	8.7	—	N.D.	—	—	15.3	N.A.	2.05
MF20	0	5.8	1.48	0.51	4.6	5.2	5.7	—	N.D.	—	—	10.9	N.A.	1.70
MF4	0	8.9	1.84	0.68	5.9	—	8.9	—	N.D.	—	—	15.8	N.A.	2.29
Le Puy	0	4.8	1.33	0.42	3.1	3.5	4.3	—	N.D.	—	3.6	9.5	N.A.	1.25
RM35D	7	5.8	1.54	0.41	5.6	5.6	5.4	—	N.D.	—	3.9	8.5	N.A.	1.27
T9	20	3.5	1.18	0.18	3.2	3.6	3.2	—	N.D.	2.7	2.7	4.0	N.A.	0.57
M10	31	2.9	1.00	0.14	3.0	2.8	3.0	—	N.D.	—	2.2	3.4	N.A.	0.46
MB	38	3.5	1.14	0.20	3.3	3.2	3.2	—	N.D.	—	1.8	4.6	N.A.	0.60
DV4	45	2.7	0.93	0.12	2.8	2.6	2.8	—	N.D.	2.1	2.1	3.8	N.A.	0.35

Key: %S = percentage of expandable layers prior to PVP intercalation; $\overline{T}_e$ = extrapolated, area-weighted mean thickness (BWA method) of fundamental illite particles measured using the reflection orders listed; α and β^2 = lognormal parameters for the distribution of fundamental particle thicknesses measured by the BWA method for 001 reflections; $\overline{T}_c$ = extrapolated mean thickness (BWA method) determined from data for the 005 reflection, corrected for strain using the 001, 002, 003 and 005 reflections; strain = root mean square of the strain determined from the same reflections; $\overline{T}_{TEM}$ = area-weighted mean thickness of fundamental illite particles measured from Pt-shadowed samples by TEM; N_{fix} = area-weighted mean thickness of fundamental illite particles calculated by the fixed cation method; $\overline{T}_{ev}$ = volume-weighted mean thickness of fundamental illite particles calculated from BWA-measured area-weighted thicknesses using Equation [22] in Delhez et al. (1982); $\overline{T}_i$ = area-weighted mean thickness of fundamental illite particles calculated by the integral peak width method (Drits et al. 1997); $1/i$ = reciprocal of integral peak width in reciprocal °2θ; dash = not analyzed; N.D. = not detectable; N.A. = not applicable.

method developed previously for intercalating smectite crystals (Beall et al. 1996a, 1996b), and was inspired by an earlier method that used PVP as a dispersing agent during the zonal centrifugation of soils (Francis 1973). The shapes of resulting XRD peaks, free from the effects of swelling, then are analyzed by the integral peak width and BWA methods. This technique cannot detect monolayers (elementary smectite particles), because their effect on XRD peak breadth is lost in the background. Therefore, the technique is limited to measuring the thickness of fundamental illite particles that are approximately ≥2 nm thick, which means that the method gives accurate mean thicknesses for I–S clays that are less than approximately 50% expandable.

MATERIALS AND METHODS

Na-saturated samples of diagenetic, hydrothermal and low-grade metamorphic I–S previously described (see Table 1 caption) were put into dilute suspension (1 mg clay/mL distilled water), and then mixed with aqueous solutions of polyvinylpyrrolidone (molecular weight = 10,000; hereafter referred to as PVP-10) in

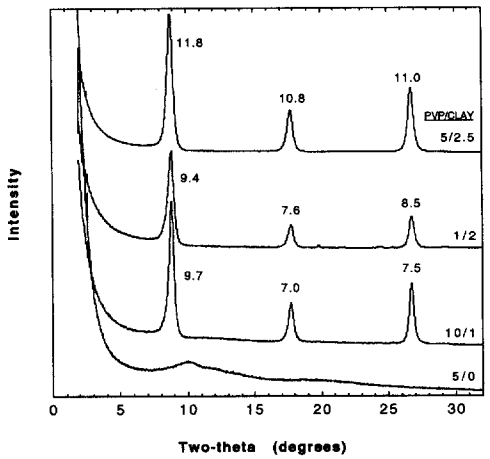

Figure 1. XRD patterns of PVP-10 intercalated sample RM30 (upper 3 patterns) showing the effect of PVP-10:clay ratio on mean particle thicknesses determined by the BWA technique. Thickness values, in nm, are displayed adjacent to the peaks. The lowermost pattern is for pure PVP-10 on a Si-substrate.

the proportion of 5 to 10 mg (solid) PVP-10 to 2.5 mg clay.

The mixtures were sonified at low power for approximately 1 min using a Heat Systems-Ultrasonics, Inc. ultrasonic probe. The mixtures (1.5 to 2 mL) then were hardened at 60 to 90 °C on 2 cm × 4 cm polished Si-metal wafers that had been cut perpendicular to (100) and glued to glass slides. The Si-substrates produce low-background XRD intensities (Li and Albe 1993), and the polished surface, together with the effects of the gel, help maximize preferred orientation of the crystals. It is evident from the XRD patterns that the illite crystals are highly oriented in the preparation, with their basal surfaces parallel to the surface of the slide, because no reflections with $hk > 0$ were observed, and because a small amount of clay (2.5 mg) often yielded large XRD intensities for 00*l* reflections. Samples were analyzed from 2 and 50 °2θ using a Siemens D500 XRD system with a diffracted beam graphite monochromator (necessary for decreasing XRD background noise), Cu*K*α radiation, and a scintillation counter. The tube current and voltage were 30 mA at 40 kV, respectively. The following slit sizes from tube to detector were used: 1°, 1°, sample, Söller, 1°, 0.15°, 0.15°. The step size was 0.02 °2θ and the count time normally was 5 s per step, but up to 20 s per step.

The resulting 00*l* XRD peaks for highly oriented illite then were measured for mean particle thickness by the integral peak-width method (Drits et al. 1997) and for mean thickness, thickness distribution and strain by the BWA method (Drits et al. 1998) using the computer program MudMaster (Eberl et al. 1996). It is important that the XRD peaks be broadened only by particle size or strain effects, and not by swelling. If swelling is present, then *d*-values of the higher order 00*l* reflections may not equal that of the first-order reflection when multiplied by the reflection order. In addition, analysis of all of the 00*l* peaks should yield the same particle thickness unless strain broadening is present. With strain broadening, calculated particle thickness (not corrected for strain) decreases regularly with increasing reflection order. Moreover, glycol solvation of PVP-10 preparations should not shift or broaden the reflections, although it may tend to decrease peak intensities by loss of particle orientation. If swelling is indicated, then the sample should be re-intercalated using a larger proportion of PVP-10.

The effects of improper preparation are obvious when an I–S sample of large expandability is prepared with too little PVP, because XRD patterns exhibit extra peaks and shoulders. Conversely, it is hard to err using too much PVP for this type of sample because XRD peaks are so broad that excess PVP has little effect on peak broadening. The effects of sample preparation on I–S of small expandability are more subtle (Figure 1). An XRD pattern for a properly prepared sample of small expandability (2%) is given in the upper pattern (Figure 1), for which the ratio of PVP-10 to clay is the recommended 2:1. All peaks give approximately the same mean thickness (11 nm) when analyzed by the BWA technique. However, if the ratio of PVP-10 to clay is too small, illite particles may not intercalate completely, resulting in XRD peaks broadened by swelling related to interparticle diffraction effects, as is demonstrated in the second pattern in Figure 1 (ratio PVP:clay = 1:2). By contrast, if the ratio is too large (10:1 ratio in Figure 1), then diffraction from the excess PVP structure itself (bottom pattern in Figure 1) may lead to a broadening of XRD peaks. Visual inspection also can be used to determine the quality of sample preparation: the intercalated clay should be invisible in the hardened gel.

The BWA method requires analysis of a sample's interference function, which is extracted from XRD intensities by dividing the intensities by the Lorentz-polarization and layer structure factors (LpG^2; Drits et al. 1998). The layer structure factor for PVP-saturated illite has not been determined theoretically; therefore an approximate LpG^2 factor was devised by using a weighted sum of a normalized, experimental, PVP-smectite LpG^2 factor for illite particle basal surfaces, and of a calculated illite LpG^2 factor for particle interiors. A previous approach for analyzing MacEwan crystallites which used a calculated LpG^2 factor corrected for the K-content of the mixed-layer crystal (Drits et al. 1998) did not work for thin (<8 nm) PVP-saturated illites, because on division of the experimental intensities by the calculated LpG^2 factor the resulting interference function became too distorted to an-

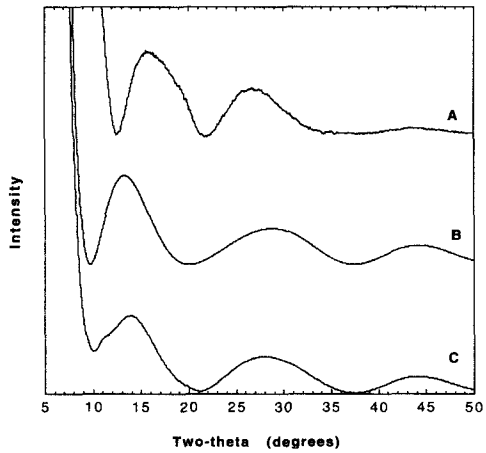

Figure 2. A = an experimental LpG² factor for PVP-intercalated, Na-Kinney montmorillonite; B = calculated LpG² factor for illite having 0.89 K per $O_{10}(OH)_2$; C = weighted mixture of the LpG² factors found in A and B according to Equation [1] in the text, for an illite sample having a mean thickness of 5 nm.

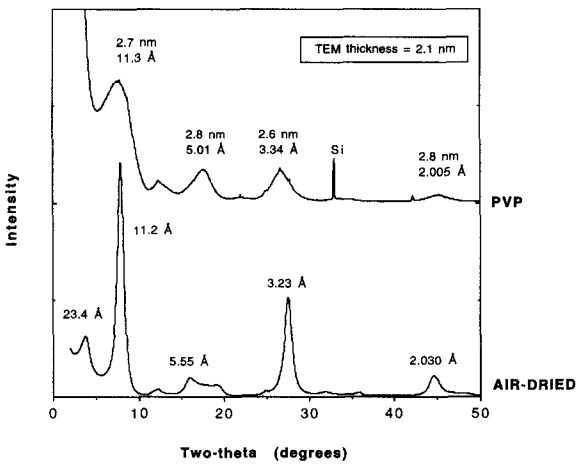

Figure 3. XRD patterns for sample DV4, normally a 45% expandable, R1-ordered I–S. Mean illite fundamental particle thicknesses measured for each 00*l* reflection by the BWA technique for the upper, PVP-intercalated sample, are labeled in nm units. Peak positions are labeled in Å units. Si = a weak peak at d = 2.715 Å which is the Renninger double diffraction of (200) for the Si-metal substrate (according to Li and Albe 1993).

alyze. Evidently PVP-10 is absorbed on illite surfaces and diffracts as a part of the structure.

Calculation of an LpG² factor for illite containing 0.89 K per $O_{10}(OH)_2$ was calculated by a standard method (Moore and Reynolds 1989, using 1-dimensional atomic structures given in their Tables A.3 and A.4) using a program named CalcLpG2, which was written as a Microsoft Excel spreadsheet (available from D. D. Eberl). An LpG² factor for a PVP-smectite-Si metal substrate sample was measured using 2.5 mg of a <1.0 μm sample of Na-Kinney montmorillonite (Khoury and Eberl 1981) which was completely intercalated with 10 mg PVP. An XRD pattern for PVP on an Si substrate was subtracted from the PVP-smectite-Si pattern to remove the effects of excess PVP and of the Si-background. The intensity maximum between 12 and 20 °2θ for this corrected pattern then was normalized to a similar intensity maximum for a calculated LpG² factor for smectite with 2-H_2O having a layer charge of 0.66 (calculated in the same manner as the illite LpG² factor using the CalcLpG2 program). This LpG² factor is used as a reference for intensity normalization because it strongly resembles the PVP-smectite pattern in that both patterns have the same general shape and both approach zero at the same 2θ values. The resulting pattern then was smoothed using an exponential smoothing function (smoothing constant = 0.8) in the Microsoft Excel 5.0a program. The resulting modified experimental LpG² factor (Figure 2A) then was applied to correct the calculated illite LpG² factor (Figure 2B) for PVP-smectite basal surfaces (Figure 2C) by using an average of the 2 LpG² factors that was weighted according to mean crystal thickness ($\bar{T}$):

$$(\mathrm{LpG}^2)_{\text{PVP-illite}} = (1 - A)(\mathrm{LpG}^2)_{\text{PVP-smectite}} + A(\mathrm{LpG}^2)_{\text{illite}} \quad [1]$$

where $A = (\bar{T} - 1) \div \bar{T}$. The correct value of $\bar{T}$ needed to determine the proportion of basal surfaces for the MudMaster calculation was found by iteration of the MudMaster program, using an educated guess based on integral peak width (Drits et al. 1997) for the first iteration.

The MudMaster program was run for all samples using a smoothing power of zero for first-order reflections and of 1 for higher orders, and XRD peaks were flipped according to recommendations given in Eberl et al. (1996). Generally, the extrapolated mean was found to equal the thickness distribution mean; but if the latter was larger, as sometimes occurs if Fourier coefficients are noisy at large sizes, then the distribution was truncated until the 2 means were equal (see Drits et al. 1998). This truncation procedure eliminates noise from the distribution, but does not affect the value of the extrapolated mean. Use of an instrumental standard and correction for the $K\alpha_1 - K\alpha_2$ doublet proved to be unnecessary for the range of thickness studied.

EXPERIMENTAL RESULTS

The effect of PVP intercalation on the XRD pattern of a highly expandable I–S (sample DV4) is shown in Figure 3. The lower pattern is from a sample of air-dried, mixed-layer, R1-ordered I–S having about 45% expandable layers. The upper pattern is from the same clay intercalated with PVP-10, in which the effect of interparticle diffraction, and therefore of swelling, has been eliminated. For the air-dried sample, diffraction

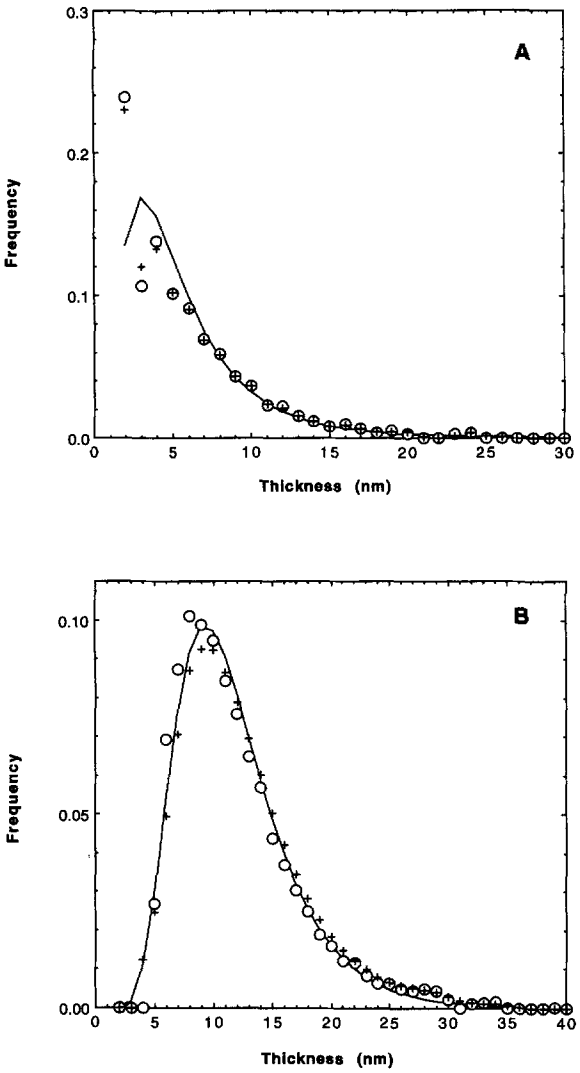

Figure 4. Fundamental illite particle area-weighted thickness distributions measured by the BWA method (without smoothing) for PVP-intercalated illites using 001 reflections (circles) compared with theoretical lognormal distributions (solid lines) and with back-calculated distributions (crosses; see text). A = asymptotic-type of distribution for sample RM35D; B = lognormal-type distribution for sample RM30.

is from stacks of fundamental illite particles and their interfaces; whereas diffraction for the PVP-10 intercalated sample is from individual fundamental illite particles. The upper pattern passes all of the tests listed previously for a nonswelling sample: each peak gives approximately the same mean particle thickness (2.7 nm) on BWA analysis, and the spacing of each peak is related by n in Bragg's Law to that of the first-order reflection (10.02 Å). The first-order reflection is so broad that it is shifted to a larger d-value (11.3 Å) by the LpG^2 factor; but when the LpG^2 factor is removed by division, the spacing of the 001 peak shifts to 10.03 Å. Glycol solvation (not shown) has no effect on the 00l reflections, other than to weaken their maximum peak intensities by decreasing particle orientation.

Experimental results for other PVP-10 intercalated I–S samples are listed in Table 1. These results include samples studied (which have been classified into 2 types based on the shapes of their thickness distributions), expandabilities (measured by XRD according to the methods of Środoń 1980, 1984); area-weighted mean thickness (measured by extrapolation using the BWA technique); lognormal parameters for thickness distributions (α and β^2); root mean square of the strain [$(\overline{\sigma_1^2})^{1/2}$ which is the standard deviation of the strain distribution; see Drits et al. 1998]; thicknesses determined from 005 reflections that have been corrected for strain ($\overline{T}_c$); 3 measures of area-weighted mean particle thickness that are independent from the BWA method, including TEM measurements of Pt-shadowed samples ($\overline{T}_{TEM}$) that have been corrected for the *ab*-area of the particles, thicknesses measured by fixed cation content (N_{fix}; Środoń et al. 1992), and area-weighted mean thicknesses measured by an integral peak-width method for the 001 reflection ($\overline{T}_i$; Drits et al. 1997); volume-weighted mean thicknesses ($\overline{T}_{cv}$) calculated from BWA-determined area-weighted thicknesses (Equation [22] in Delhez et al. 1982) for 001 reflections; and the reciprocal of the integral peak width for 001 reflections ($1/i$).

Two types of crystallite thickness distributions can be distinguished (Table 1) using the BWA technique: asymptotic, exemplified by sample RM35D (Figure 4A), and lognormal or pseudo-lognormal (approximately lognormal), exemplified by sample RM30 (Figure 4B). The circles in Figure 4 indicate the BWA-measured thickness distributions, the solid curves give the theoretical lognormal distribution calculated from these data and the crosses give back-calculated distributions, as will be discussed. Only the distribution in Figure 4B fits the theoretical lognormal curve, which is a common distribution for many types of minerals (Eberl et al. 1990). It will be shown in a future paper that the 2 crystal thickness distribution shapes likely originate from different crystal growth mechanisms; the asymptotic-type is formed by nucleation and growth in an open system with a constant nucleation rate, whereas the lognormal distribution is formed by surface-controlled growth in an open system without simultaneous nucleation.

The distributions in Figure 4 were back-calculated to insure that MudMaster can distinguish distributions having asymptotic and lognormal shapes. The distributions calculated using MudMaster from XRD peaks for the natural clays (circles) were used to calculate an XRD pattern for illite (NEWMOD© program; Reynolds 1985). The NEWMOD-calculated 001 reflections

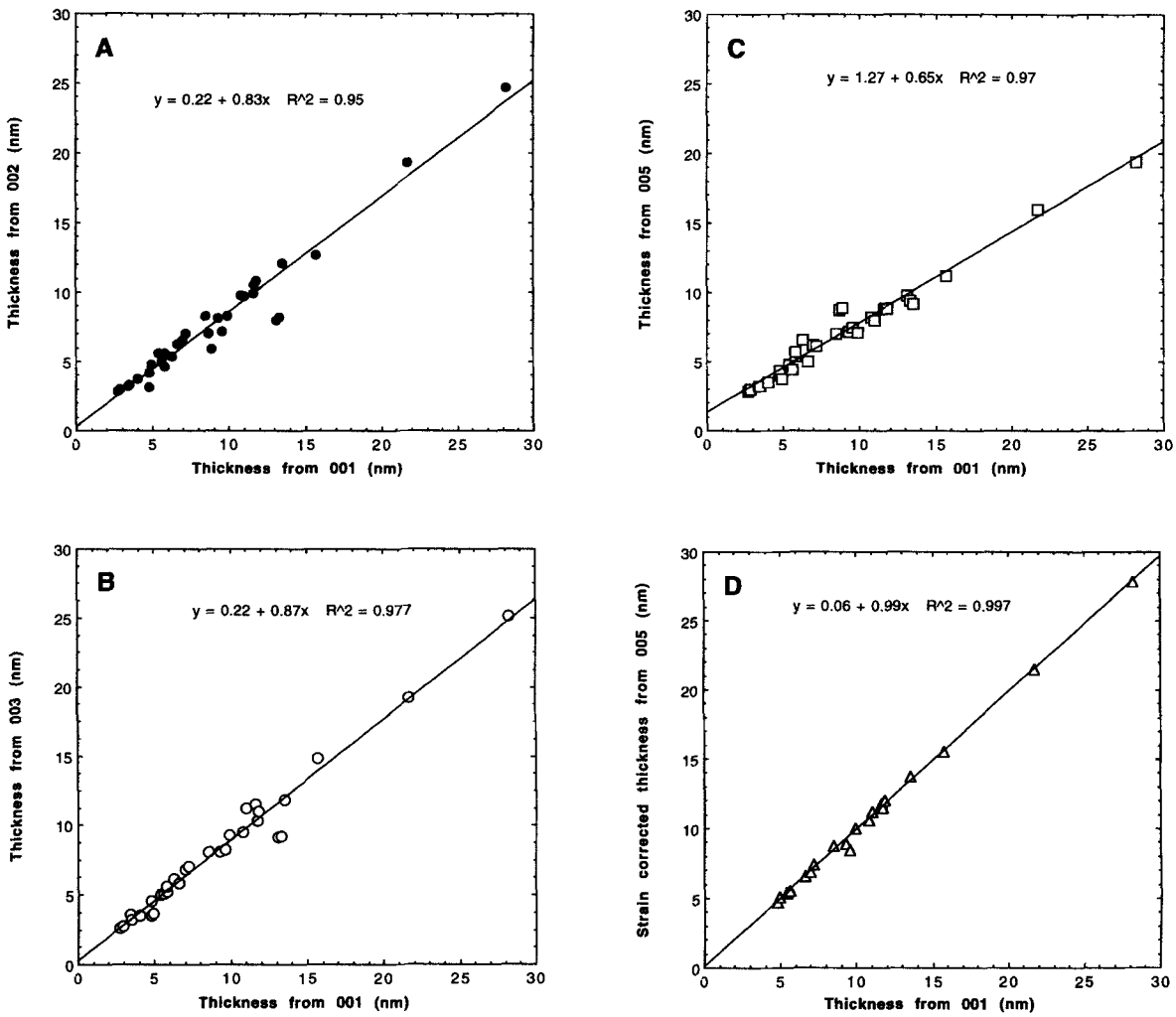

Figure 5. Extrapolated mean thicknesses measured for PVP-intercalated illites by the BWA technique for various 00*l* reflection orders (A, B, C) and for the strain corrected 005 (D, using lognormal-type illites) compared with thicknesses measured from the 001 reflection. Data from Table 1.

then were analyzed using MudMaster to give the back-calculated distributions (crosses), which closely match the experimental distributions. It has been shown previously that many types of distributions can be determined accurately using the MudMaster program (Drits et al. 1998).

Fundamental illite particle mean thicknesses ($\overline{T}_c$ and $\overline{T}_c$) measured by the BWA method for 00*l* reflection orders greater than 1 are compared to those measured by the same method for the 001 reflection in Figure 5. The relations are linear, but higher-order reflections (Figures 5A, B and C) generally give smaller mean thicknesses than do the 001 reflections. This pattern is expected if strain is present within fundamental illite particles. Mean thicknesses calculated for strained illites from 005 reflections can be corrected almost exactly by the BWA method to equal mean thicknesses calculated from the 001 reflections (Figure 5D).

The root mean square of the strain $(\overline{\sigma_l^2})^{1/2}$ varies from zero to 0.20 Å between samples, and bears no systematic relation to mean illite particle thickness (Table 1). MudMaster calculations show that $(\overline{\sigma_l^2})^{1/2}$ for most samples is constant with distance within fundamental illite particles, thereby indicating that the strain (ϵ_l) distribution for each of these samples is Gaussian (Drits et al. 1998). Strain is rare in illites having asymptotic-type crystallite thickness distributions (Table 1).

Illite particle thicknesses measured by the BWA method are compared with those measured by TEM from Pt-shadowed samples and by the fixed cation method (Figure 6). The TEM method gives slightly larger mean thicknesses in comparison to the BWA

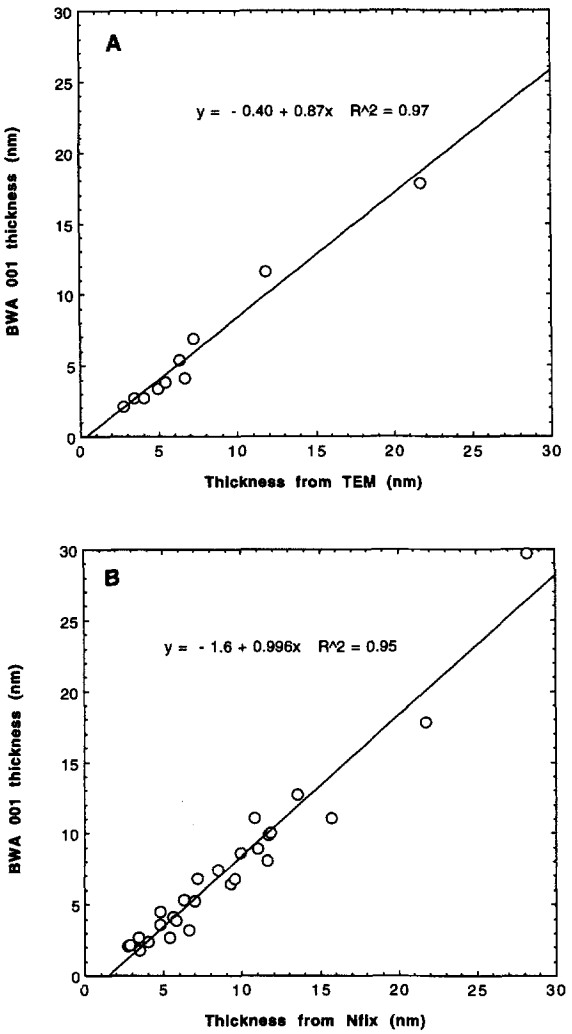

Figure 6. Mean thicknesses measured by the BWA method for PVP-intercalated illites for the 001 reflection compared with thicknesses measured by TEM Pt-shadowing (A) and by the Nfix method (B).

method, although the data are sparse. The fixed cation method also yields slightly larger (by about 1.6 nm) mean thicknesses (Figure 6B).

A plot of thicknesses measured for lognormal-type PVP-dispersed samples by the BWA method and by the integral peak width method for 001 reflections (Figure 7) indicates that the latter method, which was developed using a specific model for the evolution of mean particle thickness with lognormal distribution shape (Drits et al. 1997), gives slightly larger mean thicknesses. Mean thicknesses calculated by the BWA method require no assumptions concerning the shapes of thickness distributions. New empirical relations are given in the equations in Figure 8, in which BWA mean thicknesses calculated for 001 reflections are plotted against the reciprocal of integral peak widths

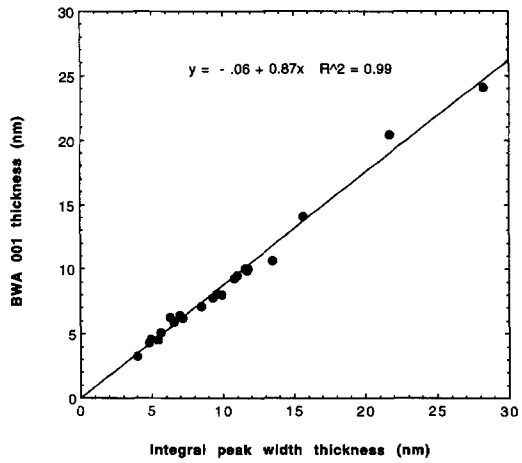

Figure 7. Mean thicknesses measured by the BWA method for PVP-intercalated illites for the 001 reflection compared with thicknesses measured by the integral peak width method of Drits et al. (1997).

(the reciprocal = maximum intensity/integrated intensity). These equations are a simpler alternative for determining mean illite thickness from integral peak width data than is the method described by Drits et al. (1997), and they take into account the 2 types of thickness distribution shapes. Figure 9 correlates BWA-calculated area-weighted means with corresponding volume-weighted means (Delhez et al. 1982) for the 2 types of distributions.

SUMMARY

Accurate measurement of fundamental illite particle thicknesses from XRD peak shape requires minimizing the effects of clay swelling and of XRD background during XRD analysis. This measurement is accomplished by intercalating dispersed, Na-saturated I–S with PVP-10, and

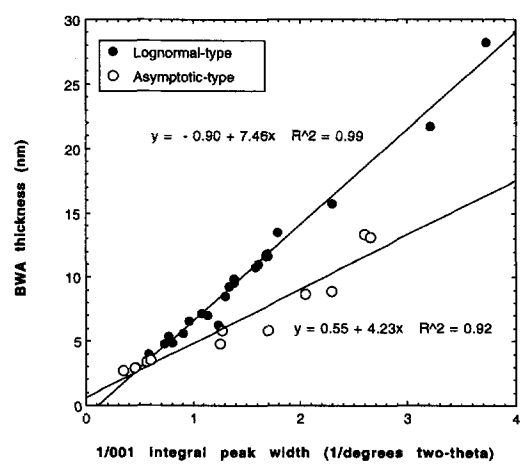

Figure 8. Mean thicknesses measured by the BWA method using the 001 reflection for PVP-intercalated illites compared with the reciprocal of the integral peak width.

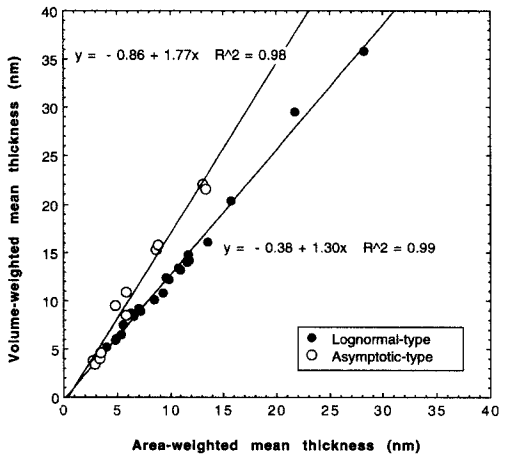

Figure 9. Area-weighted versus volume-weighted mean thicknesses determined from 001 reflections by the BWA technique.

by mounting the specimens on metallic Si substrates. Investigation of a variety of diagenetic, hydrothermal and low-grade metamorphic illites demonstrates that there are at least 2 distinct shapes for illite fundamental particle thickness distributions, asymptotic and lognormal. Strain is rare in the asymptotic-type, and generally has a Gaussian distribution in the lognormal-type. Illite fundamental particle mean thicknesses can be measured from PVP-10 intercalated samples by the integral peak width method, by the BWA method or by empirical equations given in Figure 8. The 001 reflection is best used for particle thickness determinations because it is least affected by strain, which tends to lower the measured mean thickness with increasing reflection order. However, accurate thicknesses can be determined from higher-order reflections if these measurements are corrected for strain broadening.

ACKNOWLEDGMENTS

This study was partly supported by the U.S.–Slovak Science and Technology Program, Project No. 92029. We thank D. Balzar, V. Drits, P. Nadeau, J. Neil, D. Peacor, R. Pollastro, J. Środoń and Gene Whitney for reviewing the original manuscript. The use of trade names is for identification purposes only and does not constitute endorsement by the U.S. Geological Survey.

REFERENCES

Altaner SP, Weiss CA Jr, Kirkpatrick RJ. 1988. Evidence from 29Si NMR for the structure of mixed-layer illite/smectite clay minerals. Nature 331:699–702.

Árkai P, Merriman R, Roberts B, Peacor D, Tóth M. 1996. Crystallinity, crystallite size and lattice strain of illite-muscovite and chlorite: comparison of XRD and TEM data for diagenetic to epizonal pelites. Eur J Mineral 8:1119–1137.

Beall G, Tsipursky S, Sororcin A, Goldman A. 1996a. Intercalates and exfoliates formed with oligomers and polymers and composite materials containing same. US Patent No. 5,552,469.

Beall G, Tsipursky S, Sororcin A, Goldman A. 1996b. Intercalates; exfoliates; process for manufacturing intercalates and exfoliates and composite materials containing same. US Patent No. 5,578,672.

Delhez R, de Keijser ThH, Mittemeijer EJ. 1982. Determination of crystallite size and lattice distortions through X-ray diffraction line profile analysis. Anal Chem 312:1–16.

Drits VA, Eberl DD, Środoń J. 1998. XRD measurement of mean thickness, thickness distribution and strain for illite and illite–smectite crystallites by the Bertaut-Warren-Averbach technique. Clays Clay Miner 46:38–50.

Drits VA, Środoń J, Eberl DD. 1997. XRD measurement of mean crystallite thickness of illite and illite/smectite: Reappraisal of the Kubler index and the Scherrer equation. Clays Clay Miner 45:461–475.

Eberl DD, Blum A. 1993. Illite crystallite thickness by X-ray diffraction. In: Reynolds RC Jr, Walker JR, editors. CMS Workshop Lectures, Vol. 5, Computer applications to X-ray powder diffraction analysis of clay minerals. Boulder, CO: Clay Miner Soc. p 124–153.

Eberl DD, Drits V, Środoń J, Nüesch R. 1996. MudMaster: A program for calculating crystallite size distributions and strain from the shapes of X-ray diffraction peaks. U.S. Geol Surv Open File Report 96–171:44 p.

Eberl DD, Środoń J, Lee M, Nadeau PH, Northrop HR. 1987. Sericite from the Silverton caldera, Colorado: Correlation among structure, composition, origin, and particle thickness. Am Mineral 72:914–934.

Eberl DD, Środoń J, Kralik M, Taylor B, Peterman ZE. 1990. Ostwald ripening of clays and metamorphic minerals. Science 248:474–477.

Francis CW. 1973. Adsorption of polyvinylpyrrolidone on reference clay minerals. Soil Sci 115:40–54.

Hunziker JC, Frey M, Clauer N, Dallmeyer RD, Friedrichsen H, Flehmig W, Hochstrasser K, Roggwiler P, Schwander H. 1986. The evolution of illite to muscovite: Mineralogical and isotopic data from the Glarus Alps, Switzerland. Contrib Mineral Petrol 91:157–180.

Khoury HN, Eberl D. 1981. Montmorillonite from the Amargosa Desert, southern Nevada, U.S.A. N Jb Miner Abh 141: 134–141.

Li C-T, Albe WR. 1993. Development of an improved XRD sample holder. Powder Diffraction 8:118–121.

Lindgreen H, Garnaes J, Hansen PL, Besenbacher F, Laaegsgaard E, Stensgaard I, Gould SAC, Hansma PK. 1991. Ultrafine particles of North Sea illite/smectite clay minerals investigated by STM and AFM. Am Mineral 76:1218–1222.

Merriman RJ, Roberts B, Peacor DR. 1990. A transmission electron microscope study of white mica crystallite size distribution in a mudstone to slate transitional sequence, North Wales, UK. Contrib Mineral Petrol 106:27–40.

Moore DM, Reynolds RC Jr. 1989. X-ray diffraction and the identification of clay minerals. New York: Oxford Univ Pr. 332 p.

Nadeau PH, Tait JM, McHardy WJ, Wilson MJ. 1984a. Interstratified XRD characteristics of physical mixtures of elementary clay particles. Clay Miner 19:67–76.

Nadeau PH, Wilson MJ, McHardy WJ, Tait JM. 1984b. Interstratified clay as fundamental particles. Science 225: 923–935.

Nadeau PH, Wilson MJ, McHardy WJ, Tait JM. 1984c. Interparticle diffraction: A new concept for interstratified clays. Clay Miner 19:757–759.

Reynolds RC Jr. 1985. NEWMOD©, A computer program for the calculation of one-dimensional diffraction patterns of mixed-layered clays. R. C. Reynolds, Jr., 8 Brook Dr., Hanover, New Hampshire 03755.

Środoń J. 1980. Precise identification of illite/smectite interstratifications by X-ray powder diffraction. Clays Clay Miner 28:401–411.

Środoń J. 1984. X-ray diffraction of illitic materials. Clays Clay Miner 32:337–349.

Środoń J, Elsass F. 1994. Effect of the shape of fundamental particles on XRD characteristics of illitic minerals. Eur J Mineral 6:113–122.

Środoń J, Elsass F, McHardy WJ, Morgan DJ. 1992. Chemistry of illite-smectite inferred from TEM measurements of fundamental particles. Clay Miner 27:137–158.

Sucha V, Środoń J, Elsass F, McHardy WJ. 1996. Particle shape versus coherent scattering domain of illite/smectite: evidence from HRTEM of Dolná Ves clays. Clays Clay Miner 44:665–671.

(Received 4 April 1997; accepted 8 July 1997; Ms. 97-031)